Review Article

Experimental Views of Tran-Bend Particle Deposition in Turbulent Flow with Nanoscale Effect

Kun Zhou [ID],[1] **Ke Sun** [ID],[1,2] **Xiao Jiang**,[1,3] **Shaojie Liu**,[1,2] **Zhu He** [ID],[1,2] **and Zhou Ding**[1,2]

[1]*The State Key Laboratory of Refractories and Metallurgy, Wuhan University of Science and Technology, Wuhan 430081, China*
[2]*National-Provincial Joint Engineering Research Center of High Temperature Materials and Lining Technology,*
 Wuhan University of Science and Technology, Wuhan 430081, China
[3]*Department of Mechanical Engineering, The Hong Kong Polytechnic University, Kowloon, Hong Kong*

Correspondence should be addressed to Ke Sun; randal.soon@gmail.com

This paper presented experimental views of nano- and microaerosol distribution and deposition in turbulent tran-bend flows. These views included the particle flow measurement and particle depositions through individual bends, bifurcation bends, and those behind bends. Selected experiments were summarized and compared according to the gas flow, the bend geometry, and the particle flow properties. Based on recent studies, the influencing factors of environmental humidity, particle and surface properties, nanoparticle formation, coagulation, or evolution phenomena were discussed, and then research suggestions were given for future research and applications. It is specially mentioned that the new particle formation and nanoparticle growth affect its deposition under environmental contaminant conditions; nanoscale particle dynamics and transport have a growing trend on attracting the research and industry attentions.

1. Introduction

The living environment is filled with suspended aerosol particles such as nanoparticles and PM2.5 (airborne particles with an aerodynamic diameter less than or equal to $2.5\,\mu$m) [1, 2]. These nano- and microparticles will commonly flow into enclosed places like window cracks, sampling pipes, or ventilation ducts [3]. Generally, these enclosed places own certain bends or curved ducts, which play a significant role of changing the air and particle flow directions [4, 5].

Accurate measurements of the background gas flow properties, particle properties, particle concentrations, and curved flow line geometries can accurately predict particle flow distribution, deposition, and accumulation status [6, 7]. These kinds of measurements include but not limit to gas flow velocity, wall surface roughness, particle size distribution and evolution, deposition amount, concentration distribution and evolution, and so on [8].

Hence, this article aims to review the experimental bend nano- and microparticle flow, distribution, and deposition; to analyse influencing factors; to summarize recent findings; and to give future research and application recommendations. To summarize, particle distribution and deposition in a single bend, behind a bend, and through bifurcation bends are reviewed. Selected or potential influencing parameters are discussed, including the Dean number, curvature ratio, nonspherical particle, particle evolution, particle surface effect, roughness, and environment humidity.

2. Basic Definitions

Previous studies of aerosol flow in bends focus mainly on averaged deposition and penetration. The basic aerosol deposition or loss efficiency can be expressed as follows:

$$\eta = (1 - P) \cdot 100\% = \frac{C_i - C_o}{C_i}, \tag{1}$$

where P is the particle penetration ratio or efficiency, C_o and C_i are, respectively, the mean particle mass/number concentration at the cross sections of bend exit and entrance for

a steady or periodic measurement condition. Apparently, P is reversely proportional to η, which is determined by the concentration status and related measurement technique. The commonly adopted averaged concentration C_{ave} is a convenient statistic parameter of the particle distribution description and flow status. Meantime, on the view of the statistic theory, there are also fluctuating components varying with the measurement location and the time slot. The concentration changes with the time is generally controlled by the measurement method. While for location-dependent changes, there exist particle concentration distributions, which will affect the local deposition velocity, related particle deposition distribution, and accumulation status.

Particle deposition velocity has the definition as below:

$$V_d = \frac{J}{C_{ave}}, \tag{2}$$

where J stands for a deposition flux onto a specific surface and C_{ave} denotes a mean particle concentration near a surface. An effective approach to interpret the particle deposition is to build up the relationship between the dimensionless deposition velocity V_d^+ and the dimensionless relaxation time τ_p^+. The former parameter is defined as follows:

$$V_d^+ = \frac{V_d}{u_w} = \frac{J}{C_{ave} u_w}, \tag{3}$$

where u_w is the airflow friction velocity, which is determined by the averaged or bulk flow line velocity and the friction condition of the flow lines. The background flow velocity could be easily measured by the modern apparatus. From this equation, V_d^+ is found also to be influenced by the friction condition of the flow lines, for example, the wall surface roughness.

The dimensionless relaxation time τ_p^+ mentioned above is determined as

$$\tau_p^+ = \frac{\tau_p}{\tau_e}, \tag{4}$$

where τ_e represents the eddy lifetime, which could be computed by the background flow properties. τ_p means the particle relaxation time defined by the following equation:

$$\tau_p = \frac{C_c \rho_p d_p^2}{18\mu}, \tag{5}$$

where C_c stands for Cunningham slip correction factor for particles; ρ_p and d_p are, respectively, particle density and diameter; and μ means the gas dynamic viscosity. Cunningham coefficient C_c caused by slippage is determined by the Knudsen number Kn, which is defined as the ratio between the mean free length of the air molecules and particle diameter [9]. These particle parameters can be determined from the preknown or measured background flow and particle properties.

For diffusion dominated nanoparticles, Schmidt number Sc is a crucial parameter to describe the effect of viscosity and diffusivity. It can be expressed as

$$Sc = \frac{\nu}{D_f} = \frac{3\pi\nu\mu d_p}{kTC_c}, \tag{6}$$

where ν is gas kinematic viscosity; D_f is particle diffusivity; k means the Boltzmann constant; and T stands for the temperature [10].

Along with the particle deposition expressions, the penetration efficiency P is usually depicted against the particle Stokes number St or particle aerodynamic diameter d_p. St can be formulated as

$$St = \frac{\tau_p U_{ave}}{D_h/2}, \tag{7}$$

where U_{ave} is the average air speed in the flow line like pipe, channel, or duct; and D_h is the hydraulic diameter of the flow line, given by

$$D_h = \frac{4A_c}{p_c}, \tag{8}$$

where A_c is the cross-sectional area of the flow line and p_c is the perimeter of a cross section.

For bend particle flows, additionally, the Reynolds number (Re) in flow lines is determined as

$$Re = \frac{\rho_a U_{ave} D_h}{\mu}, \tag{9}$$

where ρ_a stands for background gas density. Based on the flow line Reynolds number, the bend Dean number can be calculated by

$$De = \frac{Re}{\sqrt{R_o}}, \tag{10}$$

where R_o means the curved flow line curvature ratio. It is computed by $(r_1 + r_2)/D$, where the parameters r_1 and r_2 are inner and outside radii of the curved flow line wall, respectively. Both the Dean number and Reynolds number are useful to nondimensionally depict the bend particle flow and deposition phenomena, and they can be determined by accurate measurement of the bend geometry, background gas property, and flow velocity.

3. Particle Flow Measurement through Bends

Some experiments of particle flow focused on the velocity investigation of gas and particle phases [11–13]. Kliafas and Holt studied the average radial and streamwise velocities and related turbulent stresses in a 90° vertical to horizontal bend with a square section [11]. They adopted the laser Doppler velocimetry (LDV) and analysed the effects of Reynolds number, mass ratio, microparticle diameter, particle-wall collision, and bend deflection angles. Later, Yang and Kuan conducted similar turbulent experiments of dilute (<1% by mass loading) microsphere particle (77 μm in average) flow through a 90° horizontal to vertical bend with square section by using 2D LDV [13]. Both average and fluctuating velocities of the air and particle phases were obtained under a Reynolds number of 102,000 (bulk velocity 10 m/s). Obvious air-particle separation was observed around the bend

TABLE 1: Selected experimental studies with turbulent flow for particle deposition through bends (1986–2006).

Investigators	Pui et al. [18]	McFarland et al. [15][a]	Peters and Leith [16, 17]	Sippola and Nazaroff [19, 20][c]
Duct bends				
Bend type	Small tube	Small tube	Industrial exhaust pipe duct	Indoor rectangular ventilation duct
Deposition surface material	Round stainless steel and glass tube bends	Round wax tube bends	Bend interior coated with petroleum jelly	Bare galvanized steel and internally insulated bends
Orientation	Horizontal to downwards vertical	NR[d]	Horizontal to horizontal and horizontal to vertical	Upwards vertical to horizontal and horizontal to downwards vertical
Construction technique	NR[d]	NR[d]	Smooth, gored, and segmented	NR[d]
Hydraulic diameter, D_h (cm)	0.501 and 0.851	1.6	15.2 and 20.3	15.2
Curvature ratio, R_o (–)	5.7	1–20	1.7–12	3.01
Bend angle, θ (deg)	90	45–135	45, 90, 180	90
Air flow				
Reynolds number[b1], Re ($\times 10^3$)	6 and 10	3.2–19.8	203 and 368	21.6–88.3
Bulk velocity, U_{ave} (m·s^{-1})	18 and 31	7.7 and 18.6	20 and 27.1	2.2, 5.3, and 9.0 (8.8)
Particles				
Aerosol type and material (density) (g/cm^3)	Monodisperse liquid oleic acid (0.89)	Monodisperse liquid oleic acid (0.89)	Polydisperse glass spheres (2.45)	Monodisperse fluorescent particles (1.15)
Diameter, d_p (μm)	1.1–6.6	10	5–150	1–16
Stokes number, St (–)	0.03–1.35	0.07–0.7	0.08–16	0.00013–0.081
Reynolds number[b2], Re_p (–)	1.3–12.7	0.05–1.5	10–200	NR[d]
Dimensionless relaxation time, τ_p^+ (–)	0.4–27	0.4–23	NR[d]	0.0046–12
Comments	Assumption of no particle rebounding	Assumption of no particle rebounding	No particle rebounding using petroleum jelly	System method to reduce the effect of particle rebounding

[a]Only experimental data [15]; [b1]Reynolds number: Re = $\rho_a U_{ave} D_h / \mu$; [b2]particle Reynolds number: $Re_p = C_c \rho_p d_p U_{ave} / \mu$; [c]bend 6 in [20] is not included, and bend 5 is the downstream half of a 180° quasi-bend; [d]NR: not reported.

outer wall and so was the slip velocity. The fluctuating velocities of particle flow were found to be higher than those of airflow at the inlet of the bend.

4. Particle Deposition through Bends

4.1. Aerosol Deposition in Individual Bends. Particle deposition in pipe or duct bend sections is of potential significance, but this behavior has not been fully studied by experimental methods under turbulent flow conditions. There are limited but growing experimental investigations on bend aerosol deposition, especially in recent years as shown in Tables 1 and 2 [10, 14–24]. The scarcity of experimental work during earlier years might be attributed to the reason that both the particle deposition and distribution are comprehensive and can be varied by many factors even in straight pipe/channel/ducts [25–28].

Some existing literature of aerosol deposition from turbulent flow within bends is associated with suspended droplet studies in small diameter tubes [15, 18, 21]. Pui et al. experimentally studied the droplet flow and deposition in circular cross-sectional bends with Reynolds number Re = 6000 and 10,000 [18]. No dependence on the Reynolds number for the particle deposition efficiency was discovered. This phenomenon

was distinct from that in laminar fluid flows. McFarland et al. reported that the increased curvature ratio led the deposition efficiency to decrease. This behaviour revealed a similar trend with that in laminar flows [15]. Wilson et al. examined higher Reynolds number (Re = 10,250–30,750) and found that the Reynolds number did not obviously change deposition efficiency trends for St > 0.4 [21]. However, a remarkable increase in deposition efficiency was found for 0.1 < St < 0.4 when the Reynolds number increases.

Recently, nanoparticle deposition in bend flows has attracted a lot of research. For a tube bend flow, as demonstrated in Figure 1, Ghaffarpasand et al. measured and quantified the nanoparticle penetration efficiency in 90° bends for different Reynolds numbers (Re = 4500–10,500), Dean numbers (De = 1426–2885), Stokes numbers, and curvature ratios [24]. Agreements with Pui's empirical model were found for 12 nm and larger particles, while deviations were observed for smaller ones [18, 24]. As illustrated in Figure 2, nanoparticle deposition rates in two bends are generally higher than those in a single bend. Lin et al. investigated the penetration efficiency of nanoparticles with diameters of 8–550 nm under different laminar and turbulent flows, as shown in Figure 3 [10]. The major studied parameters included the Dean number (De = 370–950 under

TABLE 2: Selected experimental studies with turbulent flow for particle deposition through bends (2007–2018).

Investigators	Wilson et al. [21]	Ghaffarpasand et al. [24]	Sun et al. [22, 23]	Lin et al. [10]
Duct bends				
Bend type	Small tube	Small tube	Indoor rectangular ventilation duct	Small tube
Deposition surface material	Standard stainless steel (grade 304)	Stainless steel, hydraulically smooth	Galvanized steel and acrylic glass	Plexiglass
Orientation	Downwards vertical to horizontal	NR[d]	Horizontal to horizontal	NR[d]
Construction technique	Made by a standard tube bender	NR[d]	Made by university industrial center	NR[d]
Hydraulic diameter, D_h (cm)	1.02	0.48	10	1.2
Curvature ratio, R_o (–)	7.4	13.25–54	3.4	NR[d]
Bend angle, θ (deg)	90	90	90	NR[d]
Airflow				
Reynolds number, Re ($\times 10^3$)	10.25, 20.5, and 30.75	4.5–10.5 De = 1426–2885[e]	17.9, 35.6	De = 370–950[e]
Bulk velocity, U_{ave} (m·s^{-1})	15.4, 30.8, and 46.2	NR[d]	2.58, 5.14	NR[d]
Particles				
Aerosol type and material (density) (g/cm^3)	Vitamin E, that is, alpha-tocopheryl acetate (0.91)	Tungsten oxide (10.8) and ammonium nitrate (1.725)	Arizona standard test particle, basically SiO$_2$, and Al$_2$O$_3$ (2.65)	Polydisperse particles with vegetable oil
Diameter, d_p (μm)	2.2–11	0.001–0.02 (monodisperse)	0.7–100 (polydisperse)	0.008–0.55
Stokes number, St (–)	0.12–1.08	0.001–0.03	5.2×10^{-4}–0.55	NR[d]
Reynolds number[b2], Re_p (–)	NR[d]	NR[d]	NR[d]	NR[d]
Dimensionless relaxation time, τ_p^+ (-)	NR[d]	Sc = 15–820[f]	0.34–27.6	Sc = 186–268,819[f]
Comments	Assumption of no particle rebounding	Nanoparticle, neglected coagulation	With particle-wall collision	Nanoparticle mechanism considered

[e]Dean number, De = Re/$\sqrt{R_o}$; [f]Schmidt number, Sc = ν/D_f, where ν is the dynamic viscosity.

turbulent flow), Schmidt number (Sc = 186–268,819), and dimensionless bend length (l = 2–10). Combined with Taylor-series expansion method of moment (TEMOM), an empirical relationship between nanoparticle penetration efficiency and the above parameters was given. For nanoparticle deposition, turbulent and Brownian diffusions controlled particle diffusion and thus enhanced the particle deposition [29]. Nanoparticle penetration efficiency firstly increased and then decreased with the increasing of the Dean number where the penetration rate maximized at a critical Dean number. The deposition efficiency decreases with the increasing Schmidt number.

In large industrial pipe bends with the diameters of 15.2 cm and 20.3 cm, Peters and Leith studied the depositions of 5–150 μm polydisperse glass particles with particularly high Reynolds numbers (203,000 and 368,000) [16, 17]. The tested results were found to agree roughly with previous results in the literature of small tubes, and the discrepancies may come from the differences among their test conditions which included different flow conditions, configurations, and other uncertain influencing factors. In realistic experiment or application, most of these factors are strongly coupled; hence, further measurement and analysis of the particle flow and deposition characteristics in duct bends are needed.

Aerosol deposition in commonly used ventilation system in commercial or public buildings has been tested mainly in straight pipe/duct flows, considering resuspension dynamics or the whole system performance [30–32]. There are only limited experiments conducted on tran-bend particle flow behavior. Sippola and Nazaroff experimentally investigated two kinds of bends in building the ventilation system [20]. The aerosol deposition in the bend was found to be larger than that in straight ducts with fully developed turbulent flows. Sun et al. designed laboratory experiments to test the particle flow through bends made of different materials in the ventilation system [22, 23]. They discovered particle concentration distribution, deposition, and penetration phenomena and developed models on deposition velocity and penetration. These investigations above have revealed the significance of ventilation bends with noncircular cross sections considering aerosol pollution. Although there are some reported investigations, studies on particle deposition through bends with rectangular cross sections which are common in ventilation duct systems are far from fully understood.

4.2. Aerosol Deposition behind Bends. Existing studies of aerosol deposition characteristics behind bends mainly focused on the particle penetration, deposition, and the
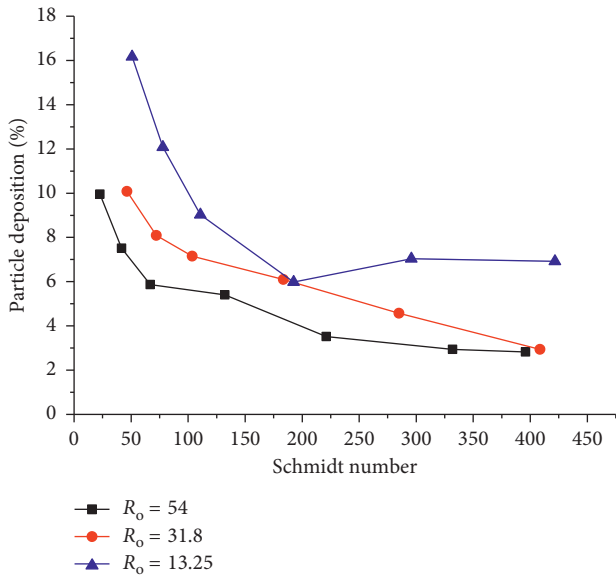
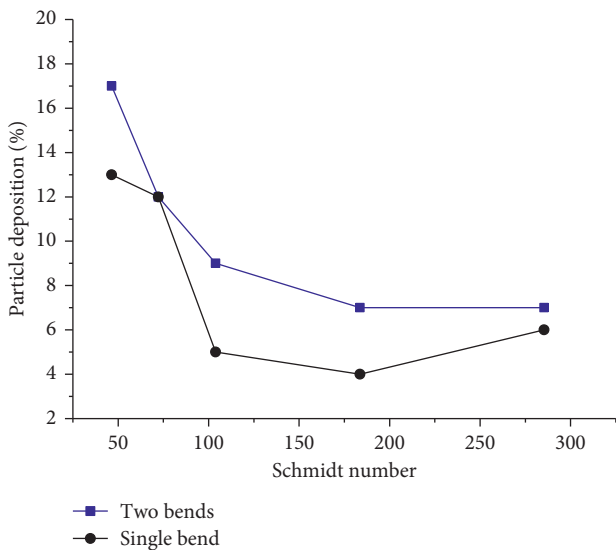FIGURE 1: Nanoparticle deposition rate varying with the Schmidt number and bend curvature ratio (R_o) [24].

FIGURE 3: Nano- and microparticle deposition rate against particle diameter under different Dean numbers [10].

FIGURE 2: Nanoparticle deposition rate varying with the Schmidt number and bend number [24].

FIGURE 4: Deposition rate of aerosol particles varying with the Stokes number (St) in different locations of the respiratory tract: ■ 1st bifurcation [34], ● 2nd bifurcation [35], and ▲ entire duct [36].

turbulent induced enhancement effects. Sippola and Nazaroff experimentally investigated two typical combined bends under various ventilation system conditions [19, 20]. The research results revealed that the particle flow and deposition behaviour behind bends were important for contaminant dispersion and fate. With experimental validation, the particle deposition phenomenon varying with the Stokes number and dimensionless distance was numerically studied behind a bend [33]. In this study, new integrated bend-induced deposition models with both those within bends and behind bends were proposed. These similar phenomena were also observed in bifurcation bend deposition in Miguel's experimental reports [34].
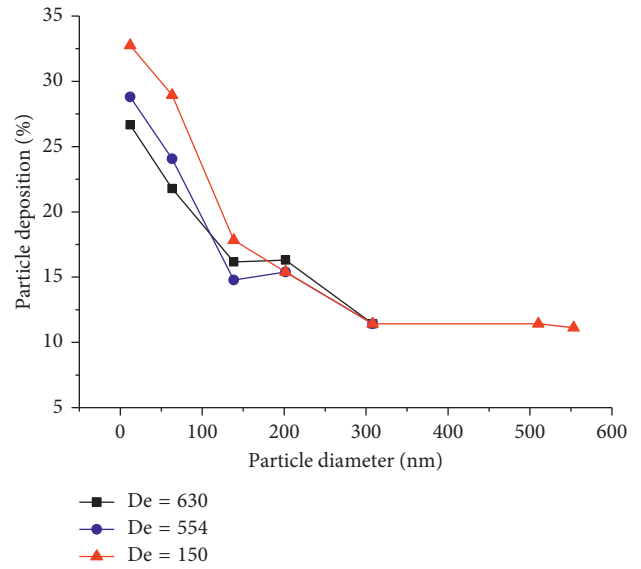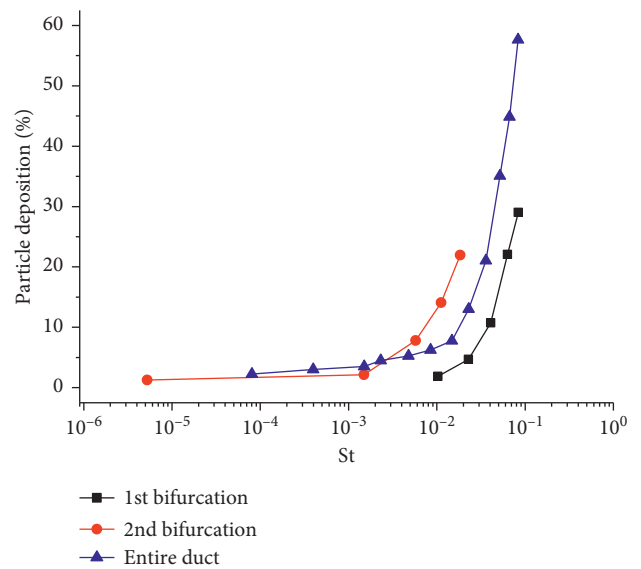
4.3. Aerosol Deposition through Bifurcation Bends.

One typical and useful application of these bend particle flows is the flow through the bifurcating system, for example, human breathing system and building ventilation system. As illustrated in Figure 4, Miguel et al. studied particle deposition in a rigid double bifurcation airway in conditions of humidity near saturation, that is, 95% (±3%) [35]. It was found that deposition increased with the particle size in the range of 0.1–9 μm, especially for coarse aerosols, which deposited more severe at the 1st bifurcation and for the obstructive-disease patient. Miguel et al. conducted another experiment to study the aerosol deposition for particles ranging from 8.1

to 23.2 μm [34, 36]. Significant factors affecting bend deposition were identified as particle size, Reynolds number, bend angle, and curvature ratio. Depositions on bifurcation segments increased with the Reynolds number. For all segments, the deposition increased with the humidity (66–95%) as well.

Rissler et al. conducted experimental determination of diesel exhaust particle (DEP) deposition in the human respiratory tract [37]. They found that the dominating deposition mechanism of particles below 500 nm was diffusion, and the diffusivity was independent of the particle effective density and a function of mobility diameter. Penconek and Moskal experimentally studied the nanosized-aggregate DEP depositions in a cast of the human respiratory system under two breathing patterns for three typical kinds of diesel fuels [38]. The results reflected that the DEP depositions varied largely with the DEP source or fuels. Depositions of particles generally increased with the tidal volume and breaths per minute.

4.4. Particle Distribution and Deposition through Bends.
Particle deposition is affected by its concentration, which could be seen in (2). For the convenience and simplicity, the averaged or uniform particle concentration is generally assumed in previous experimental, analytical, or semi-empirical investigations. However, when the fully developed turbulent flow is disturbed by some obstacles, such as bends, then flow vortex and uneven particle concentration will form accordingly [27, 28, 39]. In contrast to the averaged deposition behaviour, the new localized deposition velocity will be important, and there will be different deposition distribution patterns. For instance, Miguel et al. demonstrated that the main particle accumulation happened near the carinal ridge of each bend and the bifurcation not far from the bend [34, 35].

To analyse the deposition distribution, the particle flow and concentration behaviour through bends are important. Due to the bend effect, the flow streamlines are changed, and flow patterns, eddies, and particle pathlines are varied. A typical phenomenon is the formation of the "particle-free zone" and the "particle rope" throughout the bend. For example, Yang and Kuan showed there were very low or even void particle concentration around the bend inner wall [13, 22, 23]. These "particle-free zone" and "particle rope" confirm the above different concentration distribution, consequent different deposition distribution, and particle accumulation [40].

5. Influencing Analysis of Bend-Induced Deposition

5.1. Nonspherical Particle Effect.
With the assumption of spherical aerosols, a large number of particle deposition experiments are conducted and analysed in the literature. However, realistic aerosols are nonspherical, which would influence the aerosol concentration, orientation and distribution, the particle deposition speed, and settling behaviour [41, 42]. For instance, Lai et al. reported both

laboratory and numerical investigations on bioaerosol deposition within a ventilation chamber [43]. Better comparisons between experiment and numerical results were achieved when the nonspherical aerosol shape was considered. These findings are valuable to the future bend particle flow research.

5.2. Particle Evolution Effect.
When considering nanoparticle concentration effect to deposition distribution, the particle evolution process is one influencing factor in certain conditions with particle nucleation, coagulation, and growth [29, 44, 45]. For example, Koivisto et al. and their later study conducted size-dependent analysis of the indoor suspended particle coagulation effect on deposition behaviour [46]. It was found that this effect might vary several orders of magnitude, and it was deeply associated with the aerosol concentration and average diameter. Vohra et al. observed similar significance of including the coagulation effect in nanoparticle depositions [47]. Therefore, they recommended the consideration of the coagulation contribution in the aerosol concentration spectra change and deposition process. Due to the nanoparticle evolution mechanism, the particle size distribution changes and so is the size-dependent particle concentration distribution. The existing particle evolution studies are helpful for further investigation of the particle deposition throughout bends.

5.3. Particle-Wall Interaction Effect.
No particle re-rebound or resuspension from pipe/channel/duct surfaces is assumed in a large amount of previous experimental reports in the literature, but this assumption may not be true for solid aerosols [11, 12, 48]. One of the major mechanisms to control particle penetration/deposition is particle-wall collision [11, 48–50], which is of importance to the particle flow in two-dimensional bends. The flow differences between the particle and gas phases near the bend outer wall are caused by the particle-wall collision [13, 33]. The collision, for instance, contributes the slip velocity between the particle and gas flow, especially the enhanced transverse particle velocity behind bends. This enhanced transverse velocity may be one reason to strengthen the deposition velocity behind bends as described by Sippola and Nazaroff [20, 33]. As a result, there exist bend-induced enhancement deposition ratio and deposition velocity enhancement factor. It could also be inferred that the bend-induced developing turbulence downwards would strengthen the deposition process.

5.4. Surface Material Effect.
Furthermore, investigating the surface material effect on particle deposition in ventilation bends is important as well for understanding the particle transport in piping systems or ventilation systems [20, 22, 33]. Previous measurements with different testing materials to estimate particle penetration or deposition through bends are summarized in Tables 1 and 2. In these tables, both the bend type and particle type are listed to compare the commonly adopted bends and particles to investigate particle deposition in experimental studies. In

Table 3: Construction materials [51] applied in ventilation system.

Application field	Commercial and public buildings	Residential duct	Industrial duct	Duct for grease-laden and moisture-laden vapors	Plastic duct
Duct materials	Galvanized steel, fiberglass insulated duct, corrugated aluminum, or flexible spiral-wound Mylar [15]; iron, steel, aluminum, concrete, masonry, clay tile, fibrous glass, or G90-coated galvanized ducts	Steel, aluminum, or a material with a UL Standard 181 listing.	Galvanized steel, uncoated carbon steel, or aluminum	Carbon steel, type 304/430 stainless steel	Thermoplastic and fiberglass reinforced thermosetting ducts

detail, Sippola and Nazaroff measured the deposition through 90° ventilation bends associated with typical commercial or public mechanical ventilation systems [20]. Peters and Leith investigated industrial large pipe bends with grease coating which was considered to capture all the approaching particles [16, 17].

Nowadays, to provide a comfortable building and distinct environment, a good central ventilation system is commonly integrated in modern institutional, public, and/or commercial buildings, and the ventilation ducts have become one critical way to transport particle-laden fresh air. To construct the required ventilation ducts, many types of materials are adopted. Examples of construction materials employed in different ventilation systems are summarized in Table 3 according to ASHRAE handbooks [51] and the dissertation of Sippola [19, 51]. Several types of material steel and aluminum with different surface coatings are adopted widely, and materials with specific usage such as plastic, glass, and masonry could be seen in the table as well. Construction materials of different function ducts may play important roles in ventilation systems, and material influences on the aerosol deposition and distribution are suggested to be further studied in detail as recommended by Sippola [19].

5.5. Roughness Effect. Roughness is a factor to influence the near-wall flow and the particle-wall collision phenomena [52]. In fluid dynamics, roughness degree dominates the background friction flow or pressure loss of the pipe, duct, and channel flow [31]. For particle flow and deposition near a surface, it affects the near-wall turbulence, the flow field, and the particle-wall contact behaviour. Vohra et al. designed series of laboratory experiments to study the nanoparticle (14.3 nm–697.8 nm) deposition for different roughness surfaces under different chamber conditions [47]. They pointed out that the roughness and related turbulent flow enhanced the deposition cumulatively. It is thus inferred that the bend roughness will affect the particle distribution and deposition in the tran-bend flow process.

5.6. Turbulence Effect. Generally, the background fluid flow is fully developed before entering into the bend. With the bend effect as described by previous researchers, the flow direction is changed, developing turbulence, secondary flow, and vortexes are formed within and behind the bend [53, 54]. When vortex and turbulence are formed, different particles will have different streamlines, and uneven particle concentration, deposition, and accumulation will appear. A typical phenomenon is the formation of the "particle-free zone" and the "particle rope" throughout the bend [13, 22, 23]. From the view point of turbulent Reynolds number (Re), different experimental reports have partial consistency on the dependence between deposition efficiency and Re [18, 21, 24]. The major deviations are observed for smaller particles. For nanoparticle deposition, turbulent diffusion is one of the main factors to control particle diffusion and thus to enhance the particle deposition [29].

5.7. Moisture Effect. Moisture content in air has a positive effect on particle growth and deposition. With the increase of air humidity, particles become bigger, and depositions are increased. For example, Miguel et al. found that depositions increased with the particle size increasing from 0.1 to 23.2 μm under the humidity 66–95% (near saturation) for all segments, especially for coarse aerosols, under larger Reynolds number (e.g., Re = 1066–3151) and in the 2nd bifurcation of the respiration system [34, 35]. The deposition efficiency enhancement ranges from 10 to 35% with the humidity rising from 66% to 95%. One explanation of this phenomenon is that particles adhesion to a surface is strengthened due to humidity rise [55]. Similarly, in future study, the outdoor and indoor moisture effects on bend aerosol (e.g., PM2.5) flows are suggested to be further investigated for deeper understanding of the influencing mechanism and applications, such as the control of adverse impact of nanoparticles on human health [56].

6. Conclusions and Suggestions

This paper reviewed and analysed the investigations of particle distribution and deposition throughout the bend turbulent flow. Basic particle deposition and carrying gas flow theories were introduced at the beginning of this review work. Particle deposition and penetration formula were given to connect with the particle properties, concentrations, gas properties, flow velocities, and bend geometry and

properties. This article compared selected experimental studies on particle deposition throughout individual laboratory bends. Particle deposition through bifurcation bends was presented as well. To figure out recent and future research areas, certain influencing factors were discussed, including nonspherical particle deposition, nanoparticle evolution like coagulation, particle-wall interaction, wall surface properties, and atmospheric humidity. The study can be summarized as follows:

(1) Large amount of existing research focused on average aerosol penetration and deposition efficiency through 90° small tube bends. A wide range of curvature ratio (e.g., 1–54), Reynolds number (e.g., 3,200–368,000), particle diameter (1 nm–150 μm), particle dimensionless relaxation time τ_p^+ (e.g., 0.0046–27.6), and Schmidt number (e.g., 15–268,819) were investigated.

(2) Recently, nanoparticle with particle formation and evolution are attracting the researchers to study its penetration and deposition phenomena. It is found that aerosol deposition (e.g., nanoparticle) through bifurcation bends like respiration tract increases with the environmental humidity.

(3) Bend-induced disturbed turbulence and particle concentration lead to deposition distribution, such as the ones near the outlet of bifurcation bends. They also lead to the formation of "free-particle zone" and "particle rope." Recent integrated bend-induced deposition with both those within bends and behind bends is proposed for future possible validation and usage.

Based on these review works, suggestions or recommendations for future study and application are given below:

(1) Nonspherical particle (e.g., fiber, combustion soot, and fractal aggregate) deposition behaviour is suggested to be studied throughout the bend flow since it may influence the particle orientation, distribution, concentration, and deposition status.

(2) The new nanoparticle formation, evolution, or growth are also important mechanism for particle concentration, distribution, and deposition changes, especially under high initial concentration, large temperature-difference mixing, strong turbulence mixing, and atmospheric secondary aerosol formation or aging conditions.

(3) Wall surface roughness is another important factor to affect the bend fluid flow, near-wall turbulence, collision behavior, and thus influence the particle flow, deposition, and resuspension phenomena.

(4) Developing turbulence effect on nanoparticle diffusion and deposition is recommended to be experimentally discovered since it would be coupled with other mechanisms like nanoparticle coagulation or breakage.

(5) Tran-bend particle distribution and deposition is investigated by limited laboratory measurements. This phenomenon is typical and important to understand the bend-induced developing turbulence, particle evolution, particle deposition, and accumulation processes.

(6) Environmental humidity effect on nano- and microparticle deposition and coagulation is significant but far from fully understood. Connecting with tranbend flow, the humidity influence is suggested to be identified.

Conflicts of Interest

The authors declare that there are no conflicts of interest regarding the publication of this paper.

Acknowledgments

References

[1] X. Niu, S. S. H. Ho, K. F. Ho et al., "Indoor secondary organic aerosols formation from ozonolysis of monoterpene: an example of d-limonene with ammonia and potential impacts on pulmonary inflammations," *Science of The Total Environment*, vol. 579, pp. 212–220, 2017.

[2] M. Yu, J. Lin, and T. Chan, "Effect of precursor loading on non-spherical TiO$_2$ nanoparticle synthesis in a diffusion flame reactor," *Chemical Engineering Science*, vol. 63, no. 9, pp. 2317–2329, 2008.

[3] Y. Zhang, T. L. Chia, and W. H. Finlay, "Experimental measurement and numerical study of particle deposition in highly idealized mouth-throat models," *Aerosol Science and Technology*, vol. 40, no. 5, pp. 361–372, 2006.

[4] Q. Li, J. Song, C. Li, Y. Wei, and J. Chen, "Numerical and experimental study of particle deposition on inner wall of 180° bend," *Powder Technology*, vol. 237, pp. 241–254, 2013.

[5] X. C. Cong, G. S. Yang, J. H. Qu, and J. J. Zhao, "A model for evaluating the particle penetration efficiency in a ninety-degree bend with a circular-cross section in laminar and turbulent flow regions," *Powder Technology*, vol. 305, pp. 771–781, 2017.

[6] A. Soldati and C. Marchioli, "Physics and modelling of turbulent particle deposition and entrainment: review of a systematic study," *International Journal of Multiphase Flow*, vol. 35, no. 9, pp. 827–839, 2009.

[7] A. K. Vester, R. Orlu, and P. H. Alfredsson, "Turbulent flows in curved pipes: recent advances in experiments and simulations," *Applied Mechanics Reviews*, vol. 68, no. 5, p. 050802, 2016.

[8] P. A. Baron, P. Kulkarni, and K. Willeke, *Aerosol Measurement: Principles, Techniques, and Applications*, Wiley, Hoboken, NJ, USA, 3rd edition, 2011.

[9] W. C. Hinds, *Aerosol Technology: Properties, Behavior, and Measurement of Airborne Particles*, Wiley, New York, NY, USA, 2nd edition, 1999.

[10] J. Lin, Z. Yin, P. Lin, M. Z. Yu, and X. K. Ku, "Distribution and penetration efficiency of nanoparticles between 8-550 nm in pipe bends under laminar and turbulent flow conditions," *International Journal of Heat and Mass Transfer*, vol. 85, pp. 61–70, 2015.

[11] Y. Kliafas and M. Holt, "LDV measurements of a turbulent air-solid 2-phase flow in a 90-degree bend," *Experiments in Fluids*, vol. 5, no. 2, pp. 73–85, 1987.

[12] B. Kuan, W. Yang, and M. P. Schwarz, "Dilute gas-solid two-phase flows in a curved 90 degrees duct bend: CFD simulation with experimental validation," *Chemical Engineering Science*, vol. 62, no. 7, pp. 2068–2088, 2007.

[13] W. Yang and B. Kuan, "Experimental investigation of dilute turbulent particulate flow inside a curved 90 degrees bend," *Chemical Engineering Science*, vol. 61, no. 11, pp. 3593–3601, 2006.

[14] Q. Chen, "Comparison of different k-ε models for indoor airflow computations," *Numerical Heat Transfer Part B-Fundamentals*, vol. 28, no. 3, pp. 353–369, 1995.

[15] A. R. McFarland, H. Gong, A. Muyshondt, W. B. Wente, and N. K. Anand, "Aerosol deposition in bends with turbulent flow," *Environmental Science and Technology*, vol. 31, no. 12, pp. 3371–3377, 1997.

[16] T. A. Peters and D. Leith, "Measurement of particle deposition in industrial ducts," *Journal of Aerosol Science*, vol. 35, no. 4, pp. 529–540, 2004.

[17] T. M. Peters and D. Leith, "Particle deposition in industrial duct bends," *Annals of Occupational Hygiene*, vol. 48, no. 5, pp. 483–490, 2004.

[18] D. Y. H. Pui, F. Romaynovas, and B. Y. H. Liu, "Experimental-study of particle deposition in bends of circular cross-section," *Aerosol Science and Technology*, vol. 7, no. 3, pp. 301–315, 1987.

[19] M. R. Sippola, *Particle Deposition in Ventilation Ducts*, University of California, Berkeley, CA, USA, 2002.

[20] M. R. Sippola and W. W. Nazaroff, "Particle deposition in ventilation ducts: connectors, bends and developing turbulent flow," *Aerosol Science and Technology*, vol. 39, no. 2, pp. 139–150, 2005.

[21] S. R. Wilson, Y. A. Liu, E. A. Matida, and M. R. Johnson, "Aerosol deposition measurements as a function of Reynolds number for turbulent flow in a ninety-degree pipe bend," *Aerosol Science and Technology*, vol. 45, no. 3, pp. 364–375, 2011.

[22] K. Sun and L. Lu, "Particle flow behavior of distribution and deposition throughout 90° bends: analysis of influencing factors," *Journal of Aerosol Science*, vol. 65, pp. 26–41, 2013.

[23] K. Sun, L. Lu, H. Jiang, and H. Jin, "Experimental study of solid particle deposition in 90° ventilated bends of rectangular cross section with turbulent flow," *Aerosol Science and Technology*, vol. 47, no. 2, pp. 115–124, 2013.

[24] O. Ghaffarpasand, F. Drewnick, F. Hosseiniebalam et al., "Penetration efficiency of nanometer-sized aerosol particles in tubes under turbulent flow conditions," *Journal of Aerosol Science*, vol. 50, pp. 11–25, 2012.

[25] N. K. Anand, A. R. McFarland, F. S. Wong et al., *Deposition: Software to Calculate Particle Penetration through Aerosol Transport Systems, Report NUREG/GR-0006*, Nuclear Regulatory Commission, Washington, DC, USA, 1993.

[26] Z. Zhang and Q. Chen, "Prediction of particle deposition onto indoor surfaces by CFD with a modified Lagrangian method," *Atmospheric Environment*, vol. 43, no. 2, pp. 319–328, 2009.

[27] B. Zhao and J. Wu, "Particle deposition in indoor environments: analysis of influencing factors," *Journal of Hazardous Materials*, vol. 147, no. 1-2, pp. 439–448, 2007.

[28] B. Zhao and J. Wu, "Effect of particle spatial distribution on particle deposition in ventilation rooms," *Journal of Hazardous Materials*, vol. 170, no. 1, pp. 449–456, 2009.

[29] M. Yu, J. Lin, and T. Chan, "A new moment method for solving the coagulation equation for particles in Brownian motion," *Aerosol Science and Technology*, vol. 42, no. 9, pp. 705–713, 2008.

[30] A. C. K. Lai, "Particle deposition indoors: a review," *Indoor Air*, vol. 12, no. 4, pp. 211–214, 2002.

[31] A. C. K. Lai, M. A. Byrne, and A. J. H. Goddard, "Aerosol deposition in turbulent channel flow on a regular array of three-dimensional roughness elements," *Journal of Aerosol Science*, vol. 32, no. 1, pp. 121–137, 2001.

[32] M. R. Sippola and W. W. Nazaroff, "Modeling particle loss in ventilation ducts," *Atmospheric Environment*, vol. 37, no. 39-40, pp. 5597–5609, 2003.

[33] K. Sun, L. Lu, and H. Jiang, "A numerical study of bend-induced particle deposition in and behind duct bends," *Building and Environment*, vol. 52, pp. 77–87, 2012.

[34] A. F. Miguel, A. H. Reis, and M. Aydin, "Aerosol particle deposition and distribution in bifurcating ventilation ducts," *Journal of Hazardous Materials*, vol. 116, no. 3, pp. 249–255, 2004.

[35] A. F. Miguel, A. Reis, M. Aydin et al., "Particle deposition in airway bifurcations in different breathing conditions," *Journal of Aerosol Science*, vol. 35, no. S2, pp. 1125-1126, 2004.

[36] A. F. Miguel, "Penetration of inhaled aerosols in the bronchial tree," *Medical Engineering and Physics*, vol. 44, pp. 25–31, 2017.

[37] J. Rissler, E. Swietlicki, A. Bengtsson et al., "Experimental determination of deposition of diesel exhaust particles in the human respiratory tract," *Journal of Aerosol Science*, vol. 48, pp. 18–33, 2012.

[38] A. Penconek and A. Moskal, "Deposition of diesel exhaust particles from various fuels in a cast of human respiratory system under two breathing patterns," *Journal of Aerosol Science*, vol. 63, pp. 48–59, 2013.

[39] S. Balachandar and J. K. Eaton, "Turbulent dispersed multiphase flow," *Annual Review of Fluid Mechanics*, vol. 42, no. 1, pp. 111–133, 2010.

[40] H. Bilirgen and E. K. Levy, "Mixing and dispersion of particle ropes in lean phase pneumatic conveying," *Powder Technology*, vol. 119, no. 2, pp. 134–152, 2001.

[41] J. Wang, S. C. Kim, and D. Y. H. Pui, "Carbon nanotube penetration through a screen filter: numerical modeling and comparison with experiments," *Aerosol Science and Technology*, vol. 45, no. 3, pp. 443–452, 2011.

[42] S. Lim, H. Park, and W. G. Shin, "Experimental investigation and numerical modeling of the orientation angle of silver nanowires passing through polyester filters," *Aerosol Science and Technology*, vol. 51, no. 3, pp. 292–300, 2017.

[43] A. C. K. Lai, L. T. Wong, K. W. Mui, W. Y. Chan, and H. C. Yu, "An experimental study of bioaerosol (1–10 μm) deposition in a ventilated chamber," *Building and Environment*, vol. 56, pp. 118–126, 2012.

[44] K. Zhou and T. L. Chan, "Analytical approximation schemes for mean nucleation rate in turbulent flows," *Aerosol Science and Technology*, vol. 48, no. 5, pp. 459–466, 2014.

[45] K. Zhou, X. Jiang, K. Sun, and Z. He, "Eulerian-Lagranigan simulation of aerosol evolution in turbulent mixing layer," *Applied Mathematics and Mechanics*, vol. 37, no. 10, pp. 1305–1314, 2016.

[46] A. J. Koivisto, M. Yu, K. Hameri, and M. Seipenbusch, "Size resolved particle emission rates from an evolving indoor aerosol system," *Journal of Aerosol Science*, vol. 47, pp. 58–69, 2012.

[47] K. Vohra, K. Ghosh, S. N. Tripathi et al., "Submicron particle dynamics for different surfaces under quiescent and turbulent conditions," *Atmospheric Environment*, vol. 152, pp. 330–344, 2017.

[48] R. M. Brach and P. F. Dunn, "Models of rebound and capture for oblique microparticle impacts," *Aerosol Science and Technology*, vol. 29, no. 5, pp. 379–388, 1998.

[49] Z. F. Tian, K. Inthavong, J. Y. Tu, and G. H. Yeoh, "Numerical investigation into the effects of wall roughness on a gas-particle flow in a 90 degrees bend," *International Journal of Heat and Mass Transfer*, vol. 51, no. 5-6, pp. 1238–1250, 2008.

[50] J. Y. Tu, G. H. Yeoh, Y. S. Morsi, and W. Yang, "A study of particle rebounding characteristics of a gas-particle flow over a curved wall surface," *Aerosol Science and Technology*, vol. 38, no. 7, pp. 739–755, 2004.

[51] ASHRAE, *ASHRAE Handbook: Fundamentals*, American Society of Heating, Refrigerating and Air- Conditioning Engineers, Knovel, Atlanta, GA, USA, 2009.

[52] B. Milici, M. De Marchis, G. Sardina, and E. Napoli, "Effects of roughness on particle dynamics in turbulent channel flows: a DNS analysis," *Journal of Fluid Mechanics*, vol. 739, pp. 465–478, 2014.

[53] A. Kalpakli and R. Örlü, "Turbulent pipe flow downstream a 90° pipe bend with and without superimposed swirl," *International Journal of Heat and Fluid Flow*, vol. 41, pp. 103–111, 2013.

[54] J. A. C. Humphrey, J. H. Whitelaw, and G. Yee, "Turbulent flow in a square duct with strong curvature," *Journal of Fluid Mechanics*, vol. 103, no. 1, pp. 443–463, 2006.

[55] W. Höflinger, "Fundamentals of the compression behaviour of dust filter cakes," in *Advances in Aerosol Filtration*, K. R. Spurny, Ed., pp. 349–360, Lewis Publishers, Chelsea, MI, USA, 1998.

[56] Y. Wang, L. Chen, R. Chen et al., "Effect of relative humidity on the deposition and coagulation of aerosolized SiO_2 nanoparticles," *Atmospheric Research*, vol. 194, pp. 100–108, 2017.

The Scientific
World Journal

Journal of
Applied Chemistry

Journal of
Nanomaterials

Scientifica

International Journal of
Polymer Science

Advances in
Chemistry

Advances in
Physical Chemistry

International Journal of
Analytical Chemistry

Hindawi

Submit your manuscripts at
www.hindawi.com

Advances in
Condensed Matter Physics

Journal of
Chemistry

International Journal of
Biomaterials

Advances in
High Energy Physics

Journal of
Engineering

Journal of
Nanotechnology

International Journal of
Corrosion

Journal of
Materials

BioMed
Research International

Advances in
Tribology

Advances in
Materials Science and Engineering